ARTICLES

Investigation of CO_2/Fluorine Interactions through the Intermolecular Effects on the ^1H and ^{19}F Shielding of CH_3F and CHF_3 at Various Temperatures and Pressures

Clement R. Yonker* and Bruce J. Palmer

Environmental and Energy Sciences Division, Pacific Northwest National Laboratory, Richland, Washington 99352

Received: August 30, 2000; In Final Form: October 17, 2000

The nuclear shielding for both the ^1H and ^{19}F nuclei of CH_3F and CHF_3 was investigated as a function of pressure and temperature. The density region investigated extended from low, gaslike conditions to study pairwise intermolecular interactions to high, liquidlike densities to study multibody effects on nuclear shielding. The temperature range was from 30 to 150 °C. Neat samples of CH_3F and CHF_3, along with CO_2 mixtures of these fluorocarbons, were investigated by ^1H and ^{19}F high-pressure NMR. Molecular dynamics simulations were undertaken to describe the pair-distribution functions for both the neat samples and mixtures to aid in the interpretation of the ^1H and ^{19}F nuclear shielding determined from high-pressure NMR. The NMR spectra of the neat fluoromethanes and their CO_2 mixtures suggest that there are no distinct or specific interactions between the fluoromethanes and CO_2 and that as the temperature increases the multibody effects play less of a role in nuclear shielding.

Introduction

In the gas-phase study of the intermolecular effects on nuclear shielding, neat fluoromethanes and CO_2 solutions of the fluoromethanes are compared to determine the role of any specific CO_2/F intermolecular interactions and their perturbation on the nuclear shielding for fluorine. It has been hypothesized from the measurement of ^1H and ^{19}F chemical shifts of *n*-hexane and perfluoro-*n*-hexane dissolved in supercritical CO_2 that the chemical-shift behavior suggests a specific solute−solvent interaction between CO_2 and the fluorinated compound.[1] Ab initio calculations by Cece et al.[2] showed an enhanced interaction of CO_2 molecules with C_2F_6, in which the positively charged carbon on the CO_2 molecule intercalated between the two negatively charged fluorine atoms of a C_2F_6 molecule. The carbon dioxide molecule was slightly tilted to allow one of the oxygen atoms to interact with the positively charged carbon backbone of the hexafluoroethane. Later comments on these calculations brought into question the use of a restricted Hartree−Fock level of calculation.[3] Diep et al.[4] revisited the ab initio calculation of the interaction between CO_2 and small fluorocarbons and hydrocarbons. They reported slightly larger binding energies for the CO_2/hydrocarbon complex than for the CO_2/perfluorocarbon complex. Spectroscopic investigations of CO_2 in ethane and perfluoroethane using infrared spectroscopy by Yee et al.[5] reported no specific intermolecular interaction between CO_2 and fluorine over the pressure and temperature range investigated. The measurement of ^{19}F, ^1H, and ^2H relaxation times of perfluorobenzene, benzene, and perdeuteriobenzene in carbon dioxide over a wide range of solvent conditions failed to identify any specific interaction between fluorine and CO_2 that contributed to the molecular relaxation of this nuclei.[6]

The nuclear shielding of ^1H, ^{13}C, and ^{19}F has been extensively studied during the past 2 decades.[7−16] Nuclear shielding, σ, of the ^1H or ^{19}F nucleus in a molecule can be described by a virial expansion in density as

$$\sigma(T,\rho) = \sigma_0(T) + \sigma_1(T)\,\rho + \sigma_2(T)\,\rho^2 + ... \qquad (1)$$

where σ_0 is the rovibrational shielding of an isolated molecule at a temperature T, σ_1 is due to pairwise intermolecular interactions, and σ_2 is due to higher order multibody interactions. If one neglects the higher order terms, then the experimentally measured chemical shift of the nucleus, δ, can be related to the nuclear shielding as

$$-\delta(T) \cong (\sigma(T,\rho) - \sigma_0(T)) = \sigma_1(T)\,\rho \qquad (2)$$

In eq 2, the chemical shift has as its reference the isolated molecule, and by definition the nuclear shielding and the chemical shift are of opposite sign when measured with respect to the same reference.

The higher order terms in eq 1 can be ignored at low densities.[7,8] The pairwise shielding effects, σ_1, can then be expanded into its constituent contributions as

$$\sigma_1 = \sigma_B + \sigma_W + \sigma_a + \sigma_E = \sigma_B + \sigma_{1loc} \qquad (3)$$

where σ_B represents shielding changes resulting from the bulk magnetic susceptibility of the solvent, σ_W is the contribution to shielding from pairwise van der Waals interactions of the solute and solvent molecules, σ_a is due to the magnetic anisotropy of the solvent molecule, and σ_E is the shielding effects from the

* To whom correspondence should be addressed. E-mail: clem.yonker@pnl.gov.

10.1021/jp0031202 CCC: $20.00
Published on Web 12/16/2000

local electric fields generated near the nucleus of interest by the neighboring solvent molecules. With the exclusion of the σ_B term, the other contributions can be grouped into a single term, σ_{1loc}, and these two terms represent the pairwise contributions to the nuclear shielding. Under the assumption that σ_{1loc} is pairwise additive, the local shielding for a nucleus on molecule i can be written as

$$\rho_A \sigma_{1loc}(i) = \sum_{j=1}^{N_A} \sigma_{pair}(\tau_i, \tau_j) \tag{4}$$

where N_A is the total number of molecules of type A, ρ_A is the corresponding number density, τ_i is a generalized coordinate describing the location and orientation of molecule i, and σ_{pair} describes the shielding interaction between a pair of molecules. If eq 4 is averaged over all configurations of the solvent, it becomes

$$\sigma_{1loc}(i) = \int \sigma_{pair}(\tau_i, \tau_j)\, G(\tau_i, \tau_j)\, d\tau_j \tag{5}$$

where $G(\tau_i, \tau_j)$ is the pair-distribution function describing the relative probabilities of finding two molecules at locations τ_i and τ_j. For low values of density, this equation can be simplified further to

$$\sigma_{1loc}(i) = \int \sigma_{pair}(\tau_i, \tau_j) \exp\left(-\frac{U_{pair}(\tau_i, \tau_j)}{kT}\right) d\tau_j \tag{6}$$

where U_{pair} is the pair interaction energy. Unfortunately, from either eq 5 or 6 it can be seen that it is impossible to deconvolute information about the local interactions from a single measurement of the shielding, especially if the details of the pair-shielding function, σ_{pair}, are unknown.[7,8] However, it can be seen that a dependency of the local shielding, σ_{1loc}, on thermodynamic conditions can only enter in through the pair-distribution function $G(\tau_i, \tau_j)$, because the pair-shielding function is independent of temperature. Thus, large changes in $G(\tau_i, \tau_j)$ should lead to large changes in the shielding, and this can provide a point of contact between shielding measurements obtained by NMR and pair-distribution functions obtained from molecular dynamics simulations. Equations 5 and 6 are only applicable for neat solutions. For a mixture, they need to be modified as

$$\sigma_{1loc}^{mix}(i) = \frac{\rho_A}{\rho_A + \rho_B} \int \sigma_{pair}^{AA}(\tau_i, \tau_j)\, G_{AA}(\tau_i, \tau_j)\, d\tau_j + \frac{\rho_B}{\rho_A + \rho_B} \int \sigma_{pair}^{AB}(\tau_i, \tau_j)\, G_{AB}(\tau_i, \tau_j)\, d\tau_j \tag{7}$$

where the subscripts and superscripts refer to AA and AB pairs. Under the assumption that σ_{1loc}^{mix} is the experimental shielding of a fluorine atom measured in a fluoromethane/CO_2 mixture and σ_{1loc}^{neat} is the experimental shielding measured for the same fluorine atom in a neat fluoromethane solution, the shielding due to the interaction between the fluorine atom and the CO_2 molecules in the mixture, σ_{1loc}^{∞}, is

$$\sigma_{1loc}^{\infty} = \frac{\sigma_{1loc}^{mix} - \chi_{FM}\sigma_{1loc}^{neat}}{\chi_{CO_2}} \tag{8}$$

where χ_{FM} and χ_{CO_2} are the mole fractions of the fluoromethane and CO_2, respectively. Thus, σ_{1loc}^{∞} can be thought of as the shielding that would occur at infinite dilution in a mixture. The use of eq 8 is appropriate in the low-density regime, where eq 6 applies and the σ_{1loc}^{mix} and σ_{1loc}^{neat} values are relatively insensitive to variations in the density.

The reason for the greatly enhanced solubility of perfluorinated compounds in CO_2 as compared to that in hydrocarbons remains undetermined.[17] For this reason, the NMR chemical shifts of fluoromethane and trifluoromethane as neat solutions and dissolved in CO_2 were explored in detail. ^1H and ^{19}F nuclear shielding at low pressures over a wide range of temperatures should be sensitive to pairwise interactions between the solvent molecule and the fluoromethane. As previously mentioned, the extraction of σ_{pair} from experimental shielding data is a difficult task. This is unfortunate, because an experimentally measured σ_{pair} would play an important role in identifying specific pairwise interactions between CO_2 and fluorine in solution from relatively simple NMR experiments. As stated earlier, changes in the pairwise distribution function should lead to changes in shielding, which can be correlated with measurements obtained by NMR. Therefore, molecular dynamics calculations will be used to probe the local environment around selected nuclei in solution using potentials based on ab initio calculations of the intermolecular potential-energy surfaces developed for the fluoromethane series[18] and a model for CO_2 available in the literature.[19−21] Simulations of both the neat CH_3F and CHF_3 liquids as well as solutions with CO_2 will be performed to obtain the pair-distribution functions between different atomic sites on the molecules. The results of these simulations will be directly compared with the experimental shielding measurements to obtain a more fundamental molecular-level insight into interactions in solution and in particular the extent of any specific interaction between fluorine and carbon dioxide.

Experimental Section

High-Pressure NMR. Fluoromethane (99%) and trifluoromethane (98+%) were obtained from Fluorochem and were used without further purification. CO_2 (SFC grade, Scott Specialty Gases) mixtures with these gases were made and stored in a high-pressure, low-volume vessel. The experimental high-pressure setup and pump have been described previously.[22,23] Because of sensitivity issues at the low-pressure range investigated, ~100−800 psi, a large inner diameter capillary (324 μm i.d. × 435 μm o.d.) was used as the NMR cell in these measurements. The experimental system was evacuated before filling the capillary with the solution to be investigated. For the neat solutions of fluoromethane and trifluoromethane, the capillary NMR cell was filled directly from a syringe pump (Isco model 260D), whereas the CO_2 solutions of these molecules were loaded from the high-pressure, low-volume autoclave at room temperature. At constant temperature, the system pressure was adjusted by starting at the highest pressure investigated, usually ~800 psi, and then releasing pressure to a lower value. Therefore, the current experiments were run at constant temperature and constant mole fraction while the density was changed, as compared to the earlier efforts[11−16] in which the density was held constant while the temperature was varied. Densities for the neat fluoromethanes and their CO_2 solutions were calculated using the modified Benedict−Webb−Rubin equation of state from the National Institute of Standards and Technology (NIST) Standard Reference Database 23.[24] The mole fraction of the fluoromethanes in the CO_2 solution was between ~0.15 and 0.25 for the two molecules investigated. All spectra were acquired on a Varian (VXR-300) 300 MHz pulsed NMR spectrometer with a 7.04 T superconducting magnet. The pressure was measured using a Heise gauge with

TABLE 1: Coefficients Used To Calculate the Pairwise Additive Potentials Needed in the Molecular Dynamics Simulations

atom	$A_{ii}^{1/12}$ ((kcal mol)$^{1/12}$ Å)	$B_{ii}^{1/6}$ ((kcal mol)$^{1/6}$ Å)	$q_i(\|e\|)$
C_{CHF_3}	3.367	3.590	0.651
F_{CHF_3}	2.640	2.237	−0.233
H_{CHF_3}	1.712	0.000	0.048
C_{CH_3F}	3.285	2.760	0.339
F_{CH_3F}	2.482	2.610	−0.330
H_{CH_3F}	1.857	1.492	−0.003
C_{CO_2}	2.464	2.181	0.596
O_{CO_2}	2.912	2.813	−0.298

TABLE 2: Conditions for the Molecular Dynamics Simulations

system	N_{FM}[a]	N_{CO_2}[b]	N_{steps}
CH_3F	100		200 000
CH_3F/CO_2	25	75	200 000
CHF_3	100		200 000
CHF_3/CO_2	15	85	1 000 000

[a] N_{FM} is the number of fluoromethane molecules used in the simulation. [b] N_{CO_2} is the number of CO_2 molecules used in the simulation.

a precision of ±5 psi. The temperature was controlled to ±0.1 K, using the air bath controller on the NMR spectrometer.

Molecular Dynamics Simulations. The molecular dynamics simulations were based on pairwise additive potentials of the form

$$\phi_{ij}(r_{ij}) = \frac{A_{ij}}{r_{ij}^{12}} - \frac{B_{ij}}{r_{ij}^{6}} + a_{ij} + b_{ij}(r_{ij} - r_{cut}) + \frac{q_i q_j}{r_{ij}} \qquad (9)$$

where r_{ij} is the distance between atoms i and j, A_{ij} and B_{ij} are coefficients associated with the particular atom pair, a_{ij} and b_{ij} are constants chosen so that the interaction energy and the force due to the first two terms vanishes at the cutoff distance r_{cut}, and q_i are the partial charges associated with each of the atomic sites. Beyond the cutoff distance, only the Coulomb term contributes to the interaction. Each distinct atom i in the system is assigned a set of parameters A_{ii}, B_{ii}, and q_i. The coefficients A_{ij} and B_{ij} can then be obtained from the mixing rules $A_{ij} = (A_{ii}A_{jj})^{1/2}$ and $B_{ij} = (B_{ii}B_{jj})^{1/2}$. Atoms on the same molecule do not interact with each other. The parameters for the fluoromethane molecules were developed from ab initio calculations of the intermolecular potential-energy surfaces of the fluoromethane dimers,[18] and the parameters for CO_2 were taken from the literature.[19−21] These are summarized in Table 1.

All simulations consisted of a total of 100 molecules. The simulations of CH_3F and CO_2 contained 25 molecules of CH_3F and 75 molecules of CO_2, whereas the simulations of CHF_3 and CO_2 contained 15 molecules of CHF_3 and 85 molecules of CO_2. The equations of motion were integrated using a three-point gear predictor[25] with a time step of 2.5 fs, and a variant of the SHAKE algorithm[26] was used to maintain the internal geometry of the molecules. The long-range Coulomb interactions were handled using the Ewald summation technique, and the temperature was maintained using velocity scaling. The simulations were run for different lengths of time depending on the system; all simulations were run for long enough periods that repeatable pair-distribution functions could be obtained. A complete list of simulation conditions is provided in Table 2.

Results and Discussion

High-Pressure NMR. The shielding term, σ_1, due to pairwise interactions can be determined experimentally from the slope of the plot of the chemical shift versus density for the specific nuclei in the molecule of interest as shown in eq 2.[10] From this slope, upon correction for the bulk molar magnetic susceptibility of the solvent, one can obtain σ_{1loc}. In a superconducting magnet, σ_B is $-^4/_3\pi\chi_m$, where χ_m is the bulk molar magnetic susceptibility; therefore, $\sigma_{1loc} = \sigma_1 - (-^4/_3\pi\chi_m)$. Raynes et al.[7−10] have made compilations of ^{1}H σ_{1loc}^{neat} and $\partial\sigma_0/\partial T$, the variation with temperature of the intercept of the plot of the chemical shift versus density, for various neat hydrocarbon molecules, whereas Jameson et al.[11−16] have reported ^{19}F σ_{1loc}^{neat} and $\partial\sigma_0/\partial T$ values for numerous neat fluorocarbon molecules. Tables 3 and 4 list σ_1(slope) and σ_{1loc}^{neat} values determined in this study for both ^{1}H and ^{19}F nuclear shielding of CH_3F and CHF_3 as a function of temperature. The wide literature range reported for the σ_{1loc}^{neat} values is due to experimental error and the variance reported for χ_m values used in the calculation of σ_B. In Table 3, the ^{1}H σ_{1loc}^{neat} value of −24.0 ± 7.2 ppm cm^3 mol^{-1} for CH_3F at 30 °C compares well with the literature values for CH_3F, which range from −15.9 to −27 ppm cm^3 mol^{-1},[9] whereas the value of −5.1 ± 3.3 ppm cm^3 mol^{-1} determined for ^{1}H σ_{1loc}^{neat} of CHF_3 at 30 °C is higher than the literature values, which range from −24.3 to −35.4 ppm cm^3 mol^{-1}.[9] This discrepancy could be due to the way in which Smith and Raynes calculated the density for CHF_3, which was based on an ideal gas assumption. At room temperature, where the earlier reported experimental measurements were made, this is very close to the critical temperature for CHF_3 of 26.1 °C. Because Smith and Raynes did not report their pressure range, it could be that an ideal gas assumption was not valid, and thus their density values are in error for CHF_3, which contributes to the difference in the values reported in Table 3 for the ^{1}H σ_{1loc}^{neat} of CHF_3. In Table 4, the ^{19}F σ_{1loc}^{neat} value for CHF_3 of −150.1 ppm cm^3 mol^{-1} compares well with the literature value,[15] whereas the ^{19}F σ_{1loc}^{neat} value for CH_3F appears lower than the literature value of −307.1 ppm cm^3 mol^{-1} reported by Jameson et al.[15,27] Earlier work by Meinzer reports a ^{19}F σ_{1loc}^{neat} value for CH_3F of −451.2 ppm cm^3 mol^{-1}.[28] Our ^{19}F σ_{1loc}^{neat} value for CH_3F of −518.0 ppm cm^3 mol^{-1} compares favorably with this value.

TABLE 3: Experimental ^{1}H σ_1 and σ_{1loc}^{neat} (ppm cm^3 mol^{-1}) Values for Neat CH_3F and CHF_3 as a Function of Temperature

temp (°C)	$\sigma_1 \pm \sigma$	$\sigma_{1loc}^{neat} \pm \sigma^a$	$\sigma_{1loc}^{neat} \pm \sigma^b$
	^{1}H CH_3F		
30.0	50.6 ± 2.6	−24.0 ± 7.2	−15.9 ± 3.5
60.0	53.0 ± 0.6	−21.6 ± 3.8	
90.0	56.6 ± 0.6	−18.0 ± 3.8	
120.0	62.3 ± 0.6	−12.3 ± 3.9	
150.0	60.9 ± 1.1	−13.7 ± 5.9	
	^{1}H CHF_3		
30.0	107.6 ± 1.2	−5.1 ± 3.3	−24.3 ± 2.1
60.0	106.6 ± 2.3	−6.1 ± 4.9	
90.0	106.2 ± 0.8	−6.5 ± 2.8	
120.0	108.6 ± 1.0	−4.1 ± 3.0	
150.0	105.4 ± 1.2	−7.3 ± 3.3	

[a] The σ_{1loc}^{neat} values displayed in Table 3 are calculated using the molar bulk magnetic susceptibility reported by Smith and Raynes[9] for ease of comparison. χ_m for CH_3F is −17.8 ± 0.8 ppm cm^3 mol^{-1}, and χ_m for CHF_3 is −26.9 ppm cm^3 mol^{-1}. [b] Experimental value reported by Smith and Raynes at 20 °C.[9]

Figure 1 shows a typical plot of the experimental ^{1}H chemical shift in CH_3F versus density at constant temperature for the five temperatures investigated. By convention, nuclear shielding increases as the chemical shift decreases; therefore, the ^{1}H σ_1-values reported in Table 3 are positive. Smith and Raynes have

TABLE 4: Experimental ^{19}F σ_1 and σ_{1loc}^{neat} (ppm cm^3 mol^{-1}) Values for Neat CH_3F and CHF_3 as a Function of Temperature

temp (°C)	$\sigma_1 \pm \sigma$	$\sigma_{1loc}^{neat} \pm \sigma^a$	$\sigma_{1loc}^{neat} \pm \sigma^b$
	^{19}F CH_3F		
30.0	-429.6 ± 8.3	-518.0 ± 7.3	-307.1 ± 40
60.0	-380.7 ± 11.9	-469.1 ± 10.2	
90.0	-326.5 ± 1.6	-414.9 ± 7.0	
120.0	-312.8 ± 1.7	-401.2 ± 7.2	
150.0	-299.0 ± 1.2	-387.4 ± 6.9	
	^{19}F CHF_3		
30.0	-31.6 ± 1.5	-150.1 ± 5.6	-152.4 ± 15
60.0	-21.1 ± 0.5	-139.6 ± 3.3	
90.0	-19.0 ± 1.0	-137.5 ± 4.4	
120.0	-18.1 ± 2.2	-136.6 ± 6.7	

[a] The σ_{1loc}^{neat} values displayed in Table 4 are calculated using the bulk molar magnetic susceptibility reported by Jameson et al.[15] for ease of comparison. χ_m for CH_3F is -21.1 ppm cm^3 mol^{-1}, and χ_m for CHF_3 is -28.3 ppm cm^3 mol^{-1}. [b] Experimental value reported by Jameson et al. at 27 °C.[15]

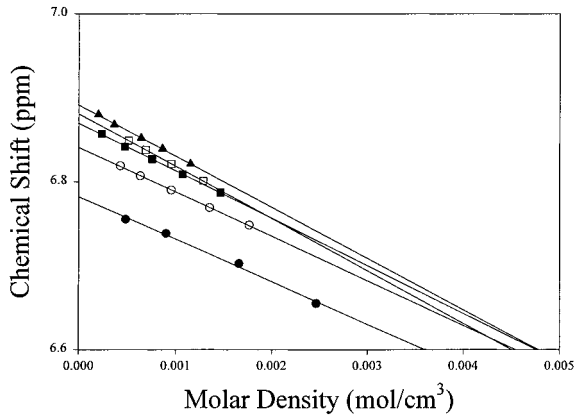

Figure 1. Plots of ^1H chemical shift (ppm) versus molar density (mol cm^3) for CH_3F at temperatures of 30 (●), 60 (○), 90 (■), 120 (□), and 150 °C (▲).

reported a trend of increasing ^1H σ_1 with increasing temperature for CH_3F.[9] Because χ_m is independent of temperature, the change in nuclear shielding for CH_3F with increasing temperature reflects a decrease in the pairwise intermolecular interactions, which results in an increase in the electron density about the ^1H nuclei, thus producing an increase in shielding. Pairwise intermolecular interactions for both ^1H- and ^{19}F-containing molecules have been shown to be deshielding in nature. For CHF_3, ^1H σ_1 shows a negligible temperature dependence, because the slope is dominated by σ_B.

Figure 2 is a plot of the ^{19}F chemical shift versus molar density for CHF_3. The ^{19}F chemical shift increases with increasing density, which is reflective of a decrease in the nuclear shielding of the fluorine nucleus as has been reported by Jameson et al.[5−10] for other fluorinated compounds. Once again, by convention, nuclear shielding increases as the chemical shift decreases; therefore, the ^{19}F $\sigma_1$values reported in Table 4 are negative. The σ_{1loc}^{neat} values listed in Table 4 become more positive with increasing temperature in a manner similar to that reported for the ^1H σ_{1loc}^{neat} values, which is indicative of pairwise intermolecular interactions being less important at high temperatures. The σ_{1loc}^{neat} value for CHF_3 at 30 °C is comparable to the value reported by Jameson et al. at 27 °C.[12,15] In contrast to this, the σ_{1loc}^{neat} value for CH_3F at 30 °C is more negative than that reported by Jameson et al. at 27 °C.[15] The reason for this discrepancy could lie in the way the earlier experiments were

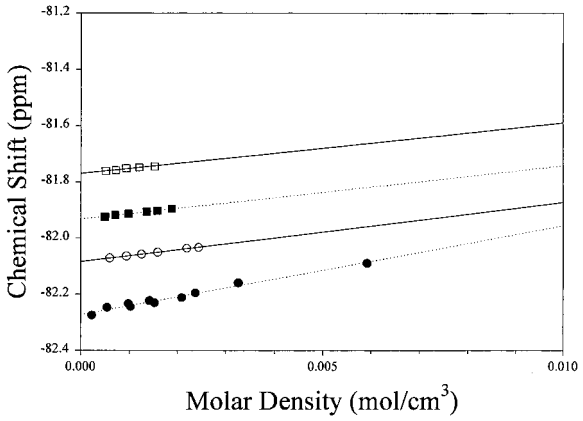

Figure 2. Plots of ^{19}F chemical shift (ppm) versus molar density (mol/cm^3) for CHF_3 at temperatures of 30 (●), 60 (○), 90 (■), and 120 °C (□).

conducted, where constant density data was collected (varying temperature) and then converted through least-squares analysis into constant temperature as a function of density.

The intramolecular effect on ^{19}F nuclear shielding in CH_3F and CHF_3 can be determined from the rovibrational change in the molecule as a function of temperature extrapolated to zero density. The *y* intercept of a plot of chemical shift versus density represents σ_0, the contribution to shielding from the rovibrational state of an isolated molecule at that specific temperature. Jameson et al. have reported $\partial\sigma_0/\partial T$ values for both CH_3F and CHF_3, which are -1.515×10^{-3} and -4.75×10^{-3} ppm K^{-1}, respectively.[13,15] The $\partial\sigma_0/\partial T$ values determined from the current experimental effort for CH_3F and CHF_3 are $-3.22 \pm 0.13 \times 10^{-3}$ and $-5.55 \pm 0.18 \times 10^{-3}$ ppm K^{-1}, respectively. The shielding of the ^{19}F nuclei changes within the molecule at higher temperatures because of the increase of the average C−F bond length as the molecule populates higher energy rovibrational states. As anticipated, the $\partial\sigma_0/\partial T$ values determined for the CO_2 mixtures were the same as those for the neat solvents.

The main contributions to the pairwise intermolecular interactions for nuclear shielding, σ_{1loc}^{neat}, of both CH_3F and CHF_3 are σ_W and σ_E. Because both molecules have large dipole moments,[29] the electric field produced at the ^{19}F nucleus from the nearby solvent molecules is most likely the dominant contribution to shielding, σ_E. These pairwise interactions should be sensitive to any specific interactions between the fluorine nucleus and the perturbing solvent molecule. Furthermore, the investigation of the binary solutions, CO_2/CH_3F and CO_2/CHF_3, could prove important in determining the role of a potential CO_2/F effect that could alter the nuclear shielding of the fluorine nucleus. Table 5 lists the experimental ^{19}F σ_1, σ_{1loc}^{mix}, and σ_{1loc}^{∞} values for CO_2/CH_3F and CO_2/CHF_3 at the temperatures investigated. σ_{1loc}^{∞} should reflect any interaction between the fluorine atom and the CO_2 molecules in the mixture at infinite dilution. For both mixtures, there are only minor differences between σ_{1loc}^{neat} and σ_{1loc}^{∞}, which is consistent with CO_2 and the fluoromethanes having comparable shielding. The similarity in the shielding suggests that there are no distinct interactions between the fluoromethanes and CO_2.

These experimental studies were in the single-phase region for the different solutions, as is evident by the lack of a liquid-phase NMR spectrum in the capillary cell,[30] whereas the higher order multibody effects could only be investigated by going to higher pressures (densities). Figure 3 shows a plot of the ^1H chemical shift normalized by the zero-density intercept as a function of density for CHF_3 (in this case an increase in $\delta - \sigma_0$

TABLE 5: Experimental ^{19}F σ_1, σ_{1loc}^{mix}, and σ_{1loc}^{∞} (ppm cm^3 mol^{-1}) Values for CO_2/CH_3F and CO_2/CHF_3 as a Function of Temperature

temp (°C)	$\sigma_1 \pm \sigma$	$\sigma_{1loc}^{mix} \pm \sigma^a$	$\sigma_{1loc}^{\infty} \pm \sigma^b$
	^{19}F CO_2/CH_3F		
30.0	−442.9 ± 1.9	−530.3 ± 11.9	−534.4
60.0	−381.3 ± 3.7	−468.7 ± 5.9	−468.6
90.0	−330.6 ± 1.7	−418.0 ± 5.4	−419.0
120.0	−305.6 ± 2.5	−393.0 ± 5.6	−390.3
150.0	−278.4 ± 5.0	−365.8 ± 7.0	−358.6
	^{19}F CO_2/CHF_3		
30.0	−38.7 ± 1.1	−133.7 ± 6.9	−130.8
60.0	−34.9 ± 1.2	−129.9 ± 7.2	−128.2
90.0	−33.4 ± 0.7	−128.4 ± 7.0	−126.8
120.0	−27.9 ± 0.8	−122.9 ± 7.1	−120.5

[a] σ_{1loc}^{mix} is determined from a χ_m value of the mixture based on the mole fraction of the two components. [b] σ_{1loc}^{∞} is determined from eq 8.

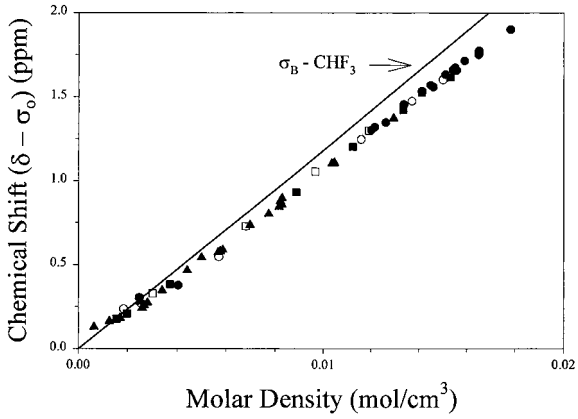

Figure 3. Plot of ^1H chemical shift (ppm) normalized by the zero-density intercept ($\delta - \sigma_0$) for CHF_3 as a function of molar density at temperatures of 30 (●), 60 (○), 90 (■), 120 (□), and 150 °C (▲). The solid line is the contribution from the bulk molar magnetic susceptibility for CHF_3.

is indicative of an increase in nuclear shielding). The solid line in Figure 3 represents the contribution from the bulk molar magnetic susceptibility to the overall change in ^1H nuclear shielding. The bulk contribution makes a >90% contribution to the nuclear shielding over the density range studied.

Of interest is the deviation from the bulk molar magnetic susceptibility for the ^1H chemical shifts of CHF_3 at high density shown in Figure 3; this could be a manifestation of multibody interactions under these conditions. However, because of the dominance of the bulk molar magnetic susceptibility on the measured chemical shift, it is difficult to assess the role of multibody interactions. To investigate this trend further, ^{19}F chemical shifts were measured for CH_3F to higher densities using a 180 μm i.d. capillary NMR cell. Figure 4 plots the ^{19}F chemical shifts for CH_3F at the two temperatures of 30 and 150 °C. At high densities (>0.01 mol cm^3), all of the chemical-shift data at the various temperatures were linear-regressed and extrapolated back to zero density. The dashed line in Figure 4 is the linear least-squares fit for all of the high-density data (only the 30 and 150 °C data points are shown for clarity). If one focuses on the chemical shifts for 30 °C in Figure 4, there is a large difference between the two extrapolations, the first extrapolation being from low to high density and the second extrapolation from high to low density. The difference is physically meaningful at high densities and represents the effect of multibody interactions on the ^{19}F chemical shift. These multibody interactions at high density are shielding in nature,

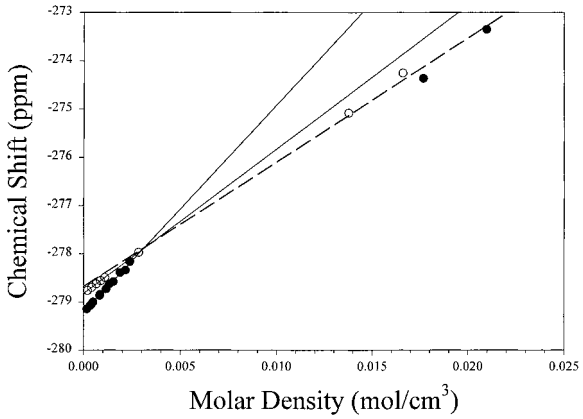

Figure 4. Plot of the ^{19}F chemical shift versus molar density for the CH_3F molecule at temperatures of 30 (●) and 150 °C (○). The dashed line is the linear regression of all of the high-density chemical-shift data for the temperatures investigated.

which supports a similar conclusion by Jameson and Jameson.[12] The other temperatures behaved in a similar manner, with the difference between the two extrapolations decreasing as a function of temperature, as shown in Figure 4 for the 150 °C data. The experimental chemical shift demonstrates that as the temperature increases the multibody effects play less of a role in nuclear shielding, as readily demonstrated by the 150 °C data. The behavior of the ^{19}F shielding of the CH_3F molecule as a function of density and temperature is dependent on the change in energy (temperature) and packing effects (density). In the gaslike region at constant density (0.000−0.004 mol cm^3), increasing temperature increases the average kinetic energy and free rotational motion of the molecule. This manifests itself through sequential changes in the chemical shift with temperature, which is not seen at the higher densities. At high density (>0.01 mol cm^3), the packing fraction increases and the solution structure becomes that of the liquid structure.

Molecular Dynamics Simulations. Molecular dynamics simulations were used to determine the pair-distribution functions between different atomic sites on the fluoromethanes for both the neat and the CO_2/fluoromethane solutions. The pair-distribution functions are of interest both as local probes of the environment around a given atom because of the solvent and because the pair-distribution function $G_{ij}(r_{ij})$ is related to the potential of mean force, $w_{ij}(r_{ij})$, via the expression

$$G_{ij}(r_{ij}) = \exp[-w_{ij}(r_{ij})/k_B T] \qquad (10)$$

The potential of mean force can be loosely thought of as the effective potential between two sites i and j when the effects of thermal motion and the surrounding solvent have been accounted for. Equation 10 suggests that significant changes in the pair-distribution function can be interpreted as changes in the effective interaction between different atomic sites. Interestingly, the pair distributions between different sites on the fluoromethane molecules show almost no change on going from the neat to the CO_2/fluoromethane solution. This is true for both CH_3F and CHF_3 and also appears to be true at different temperatures. A comparison of the C−C, F−F, and H−F pair-distribution functions between different atomic sites on CH_3F for both neat CH_3F and the CO_2/CH_3F mixture at 30 °C is shown in parts A and B of Figure 5, respectively. Although the pair-distribution functions for the mixture are a little noisier because of poorer statistics, the results are otherwise comparable. Similar results were obtained for CHF_3 and for both systems at 150 °C. Returning to eq 5, this suggests that the pair-distribution

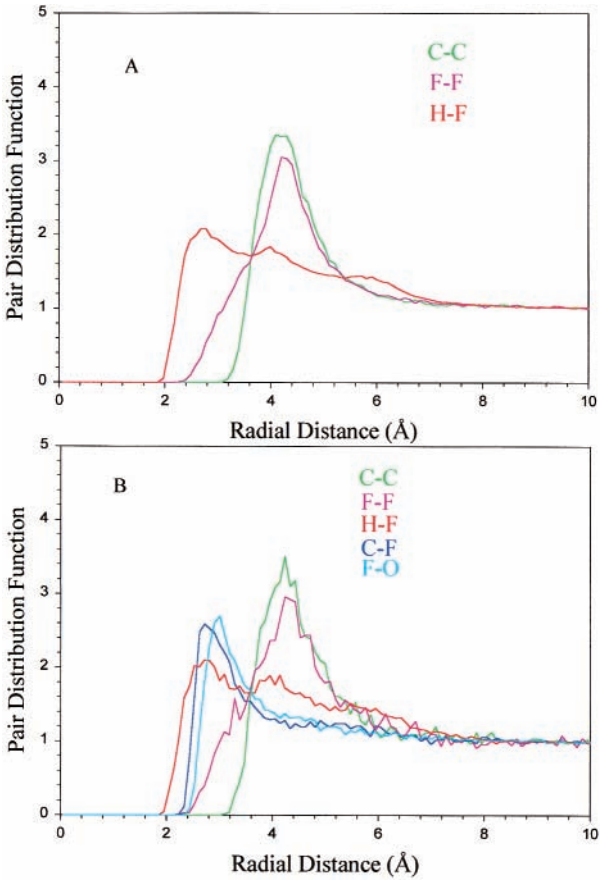

Figure 5. Pair-distribution functions for (A) neat CH_3F and (B) CH_3F/CO_2 at 30 °C. The C−C, F−F, F−H, F−C, and F−O pair-distributions functions are shown.

functions are relatively insensitive to changes in composition and density, and therefore the system is represented by eq 6 in the low-density regime. Experimentally, this implies that σ_{1loc} for the system at a given temperature and composition is relatively insensitive to density (no higher order density terms; see eq 1). This is supported by the linear behavior of the experimental chemical shifts with density as seen in Figures 1 and 2.

However, the simulations show that temperature has a very large effect on the pair distributions for the CH_3F systems and a much smaller, but still noticeable, effect on the CHF_3 system. They also show that the fluid around the atoms in CH_3F is much more highly structured than that around CHF_3. The C−C, F−F, and H−F pair-distribution functions for neat CH_3F at 150 °C are shown in Figure 6. These can be compared to the corresponding pair-distribution functions at 30 °C in Figure 5A. Note that all peaks have dropped considerably in magnitude at 150 °C. The pair-distribution functions between the fluorine and the carbon and oxygen atoms on CO_2 (C−F and F−O) in the CO_2/CH_3F mixture also show substantial structure at 30 °C (see Figure 5B), which largely disappears at 150 °C (not shown). The corresponding pair-distribution functions for neat CHF_3 at 30 and 150 °C are shown in parts A and B of Figure 7, respectively. Except for the C−C pair-distribution function, these pair-distribution functions show little structure. There is a slight drop in the functions at short distances as the temperature is increased but nothing comparable to that seen for CH_3F. The C−F and F−O pair-distribution functions for the CO_2/CHF_3 mixture exhibit similar behavior. There is little structure in the pair-distribution functions for CO_2/CHF_3 at 30 °C, and this decreases slightly as the temperature is raised. Overall, there is

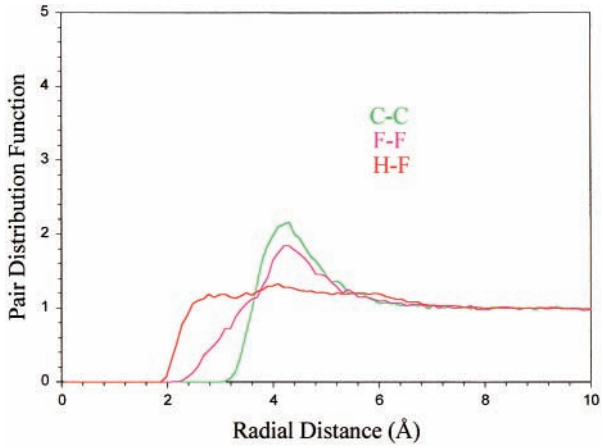

Figure 6. Pair-distribution function of CH_3F at 150 °C. The C−C, F−F, and F−H pair-distribution functions are shown.

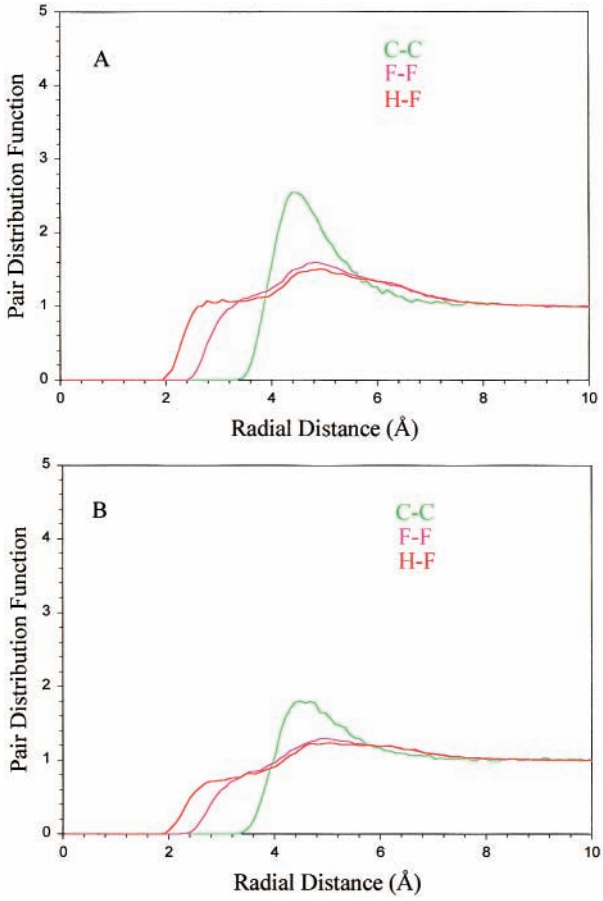

Figure 7. Pair-distribution function of neat CHF_3 at (A) 30 and (B) 150 °C. The C−C, F−F, and F−H pair-distribution functions are shown.

significantly more structure around the CH_3F molecule in solution than the CHF_3 molecule, and this structure is rapidly destroyed as the temperature is raised. This suggests that the chemical shifts in the CH_3F systems should vary significantly beyond what can be directly accounted for by differences in the bulk molar magnetic susceptibility of the system because of changes in composition and density as shown in Figure 4.

Through a comparison of Figures 5A and 7A, it can be seen that the fluoromethanes do not appear to be strongly hydrogen-bonding liquids. The H−F pair-distribution functions for both systems are relatively weakly structured, although the CH_3F system is more structured than that of CHF_3. The peak at 2.7 Å in the H−F pair-distribution function for CH_3F is probably due

to hydrogen bonding between the H and F atoms, and the weak secondary peak at 4.0 Å is probably a weak correlation between the non-hydrogen-bonding hydrogens on the donor molecule and the fluorine atom on the acceptor molecule. There is no structure for short distances in the H−F pair distribution of CHF_3, suggesting a complete absence of hydrogen bonding in this system. The fact that both systems appear to be weak hydrogen bonders indicates that the dominant interactions may be mostly steric in nature. This is also suggested by the fact that the pair-distribution functions between fluorine and the carbon and oxygen on CO_2 in the CH_3F/CO_2 mixture are very similar, indicating that the interactions between fluorine and the carbon and oxygen on CO_2 are almost the same. The differences in fluid structure around the fluoromethane molecules may be because the molecules have significantly different shapes: CH_3F is a prolate ellipsoid, whereas CHF_3 is an oblate ellipsoid. A largely steric interaction would help account for the fact that the pair-distribution functions between the fluorine atoms and the carbon and oxygen atoms on CO_2 are qualitatively the same in each of the two systems, which implies no specific CO_2/F interactions.

The NMR investigations result in two main points: (1) the similarity in nuclear shielding between σ_{1loc}^{neat} and σ_{1loc}^{∞} for the neat fluoromethanes and their CO_2 mixtures suggests that there are no distinct or specific interactions between the fluoromethanes and CO_2 and (2) the experimental chemical shift demonstrates that as temperature increases the multibody effects play less of a role in nuclear shielding. Overall, the molecular dynamics simulations apparently support these NMR conclusions. First, the simulations show that the pair-distribution functions between the different sites on the fluoromethane molecules show almost no change on going from the neat to the CO_2/fluoromethane mixture, which supports the first point stated above. This could be due to the steric nature of the overall interaction in these systems. Second, in the simulations, the structure around the CH_3F molecule in solution was rapidly destroyed as the temperature was increased. This could support the large change seen in both the ^1H and ^{19}F σ_{1loc}^{neat} experimental values for CH_3F as a function of temperature.

Conclusions

The ^1H and ^{19}F nuclear shielding for CH_3F and CHF_3 in neat and CO_2 solutions was experimentally determined and compared with previously published data. The current investigation of σ_{1loc}^{neat} compared quite favorably with previous results except for CH_3F, in which the results showed the ^{19}F nucleus in the neat solvent to be more deshielded than previously reported.[15] The NMR spectra of the neat fluoromethanes and their CO_2 mixtures suggest that there are no distinct or specific interactions between the fluoromethanes and CO_2 and that as temperature increases the multibody effects play less of a role in nuclear shielding. The molecular dynamics simulations are consistent with the behavior seen in the NMR experiments. The pair-distribution functions for CH_3F show large changes with temperature, which are consistent with the large change in σ_{1loc}^{neat} as a function of temperature seen for this system, whereas the pair-distribution functions for CHF_3 showed only minor changes with temperature, which is consistent with the temperature behavior for both the experimental chemical shift and σ_{1loc}^{neat} for this molecule. The simulations do not support any strong interaction between atom pairs, either in the neat solvent or in the mixtures. Overall, this effort helps confirm the lack of specific CO_2/fluorine interactions in solution. It remains to be determined what the mechanism of enhanced solubility of fluorinated compounds in CO_2 is.

Acknowledgment. Work at the Pacific Northwest National Laboratory (PNNL) was supported by the Office of Science, Office of Basic Energy Sciences, Chemical Sciences Division of the U.S. Department of Energy, under Contract DE-AC076RLO 1830.

References and Notes

(1) Dardin, A.; DeSimone, J. M.; Samulski, E. T. *J. Phys. Chem. B* **1998**, *102*, 1775.
(2) Cece, A.; Jureller, S. H.; Kerscher, J. L.; Moschner, K. F. *J. Phys. Chem.* **1996**, *100*, 7435.
(3) Han, Y.-K.; Jeong, H. Y. *J. Phys. Chem. A* **1997**, *101*, 5604.
(4) Diep, P.; Jordan, K. D.; Johnson, J. K.; Beckman, E. J. *J. Phys. Chem. A* **1998**, *102*, 2231.
(5) Yee, G. G.; Fulton, J. L.; Smith, R. D. *J. Phys. Chem.* **1992**, *96*, 6172.
(6) Yonker, C. R. *J. Phys. Chem. A* **2000**, *104*, 685.
(7) Bennett, B.; Raynes, W. T. *Magn. Reson. Chem.* **1991**, *29*, 946.
(8) Bennett, B.; Raynes, W. T. *Magn. Reson. Chem.* **1991**, *29*, 955.
(9) Smith, A.; Raynes, W. T. *J. Crystallogr. Spectrosc. Res.* **1983**, *13*, 77.
(10) Raynes, W. T.; Buckingham, A. D.; Bernstein, H. J. *J. Chem. Phys.* **1962**, *36*, 3481.
(11) Jameson, C. J.; Jameson, A. K.; Burrell, P. M. *J. Chem. Phys.* **1980**, *73*, 6013.
(12) Jameson, C. J.; Jameson, A. K. *J. Chem. Phys.* **1984**, *81*, 1198.
(13) Jameson, C. J. *Mol. Phys.* **1985**, *54*, 73.
(14) Jameson, C. J.; Jameson, A. K.; Oppusunggu, D. *J. Chem. Phys.* **1984**, *81*, 2313.
(15) Jameson, C. J.; Jameson, A. K.; Oppusunggu, D. *J. Chem. Phys.* **1984**, *81*, 85.
(16) Jameson, C. J.; Jameson, A. K. *J. Magn. Reson.* **1985**, *62*, 209.
(17) Laintz, K. E.; Wai, C. M.; Yonker, C. R.; Smith, R. D. *J. Supercrit. Fluids* **1991**, *4*, 194.
(18) Palmer, B. J.; Anchell, J. L. *J. Phys. Chem.* **1995**, *99*, 12239.
(19) Murthy, C. S.; Singer, K.; McDonald, I. R. *Mol. Phys.* **1981**, *44*, 135.
(20) Murthy, C. S.; O'Shea, S. F.; McDonald, I. R. *Mol. Phys.* **1983**, *50*, 531.
(21) Geiger, L. C.; Ladanyi, B.; Chapin, M. E. *J. Chem. Phys.* **1990**, *93*, 4533.
(22) Bai, S.; Yonker, C. R. *J. Phys. Chem. A* **1998**, *102*, 8641.
(23) Yonker, C. R.; Wallen, S. L.; Palmer, B. J.; Garrett, B. C. *J. Phys. Chem. A* **1997**, *101*, 9564.
(24) McLinden, M. O.; Klein, S. A.; Lemmon, E. W.; Peskin, A. P. NIST Thermodynamic and Transport Properties of Refrigerants and Refrigerant Mixtures—REFPROP. *NIST Standard Reference Database 23*, 1998.
(25) Allen, M. F.; Tildesley, D. J. *Computer Simulations of Liquids*; Clarendon Press: Oxford, U.K., 1987.
(26) Palmer, B. J. *J. Comput. Phys.* **1993**, *104*, 470.
(27) Jameson, C. J.; Jameson, A. K. *J. Chem. Phys.* **1978**, *69*, 1655.
(28) Meinzer, R. A. Ph.D. Thesis, University of Illinois, 1965 (University Microfilm, Inc., Ann Arbor, MI, No. 66-4238).
(29) Gray, C. G.; Gubbins, K. E. *Theory of Molecular Fluids, Volume 1*: *Fundamentals*; Oxford University Press: London, 1984; Appendix D.
(30) Yonker, C. R.; Linehan, J. C.; Fulton, J. L. *J. Supercrit. Fluids* **1998**, *14*, 9.